

Crystal Structure Analysis and Electron Density Distribution of Proton Conductive Layered Perovskite $\text{Sr}_2(\text{Ti}_{1-x}\text{M}_x)\text{O}_{4-\delta}$ (M = Fe, Al)

This study evaluated the influence of Fe and Al substitution on their crystal structures and the creation of proton defects in Sr_2TiO_4 -based layered perovskites. The mechanism of proton defect creation was different between Fe and Al substitutions as described in the main text. The obtained result is an important guide for dopant selection when developing new proton-conductive oxides with greater amounts of proton defects. The electron density distribution obtained from synchrotron X-ray diffraction provides a useful clue for investigating whether the proton defects are created.

Sr_2TiO_4 -based layered perovskites are an alternative candidate for potential proton conductors because titanate layered perovskites have a higher chemical stability than zirconate- or cerate-based perovskites. However, the lower proton conductivity of titanate layered perovskites remains an obstacle. To improve the conductivity, in this study we tried to increase proton defects by substituting acceptor elements and then creating oxygen vacancies in the Sr_2TiO_4 -based layered perovskites, and investigated the effects of Fe and Al as acceptor dopants on the crystal structure, oxygen vacancies and proton uptake.

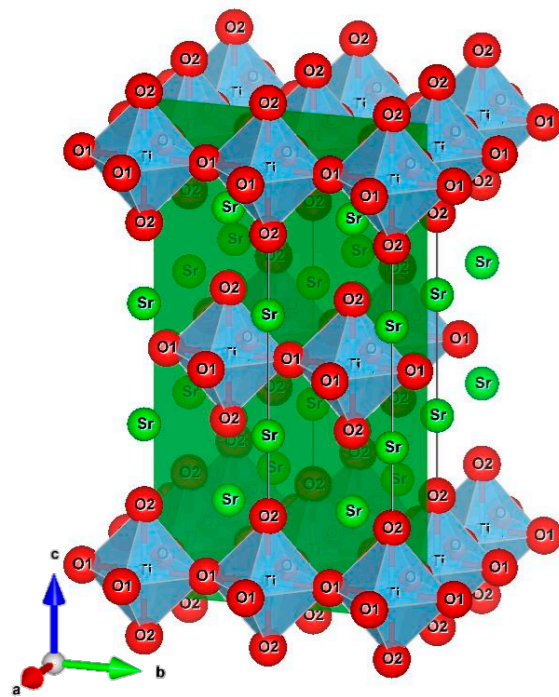


Figure 1: Refined crystal structure of as-sintered STA05 portrayed as the $2 \times 2 \times 1$ supercell of the Sr_2TiO_4 unit cell. The green plate represents the (200) plane. Reprinted from Yagi *et al.* [1] with permission from Elsevier.

$\text{Sr}_2\text{Ti}_{0.9}\text{Fe}_{0.1}\text{O}_{4-\delta}$ (STF10) and $\text{Sr}_2\text{Ti}_{0.95}\text{Al}_{0.05}\text{O}_{4-\delta}$ (STA05) ceramic samples were prepared by a solid-state reaction method [1]. The sintering conditions were 1450°C for 10 h under ambient air, which are appropriate for preparing dense samples with relative densities of $>96\%$. To introduce proton defects, the samples were annealed under dry 20% $\text{H}_2\text{-N}_2$ mixed gas (water vapor partial pressure: ~ 0.006 atm) or moist 50% $\text{H}_2\text{-N}_2$ mixed gas (water vapor partial pressure: ~ 0.02 atm) at a flow rate of 200–300 ccm at 600°C for 10–20 h. The annealed samples are referred to as “reduced sample” and “moist-reduction-annealed sample,” respectively.

Synchrotron X-ray powder diffraction (SXRPD) was carried out at BL-4B2. A high-resolution powder diffractometer with a multiple-detector system (MDS) installed at BL-4B2 was used [2]. Diffraction data were recorded in steps of 0.005° in the 2θ range from 10° to 129° at room temperature under ambient air. Incident beams with wavelengths of 1.19730(1), 1.19715(1), 1.19716(1), and 1.19722(1) Å were extracted by using a double crystal monochromator. Lattice constant and structural parameters of the prepared samples were refined by Rietveld analysis using the RIETAN-FP program [3]. The electron density distributions were calculated by the maximum entropy method.

Figure 1 illustrates the refined crystal structure of as-sintered STA05. As-sintered STF10 had a larger cell volume ($V = 190.006(1) \text{ \AA}^3$) than that of as-sintered STA05 ($V = 189.370(2) \text{ \AA}^3$) [1]. This is because the ions that were substituted into the Ti sites, namely Fe^{3+} and Fe^{4+} , have larger ionic radii (0.645 and 0.585 Å, respectively) than Al^{3+} (0.535 Å) under the coordination number of 6 [4]. The cell volume of reduced STF10 ($V = 191.131(3) \text{ \AA}^3$) [1] was larger than that of as-sintered STF10, suggesting that the annealing reduces Fe^{4+} to Fe^{3+} . The occupancy of the O1 site of STA05 increased after moist reduction annealing from 0.986(5) to 1, suggesting that proton defects are generated by dissociative incorporation of water vapor at the expense of the oxygen vacancies.

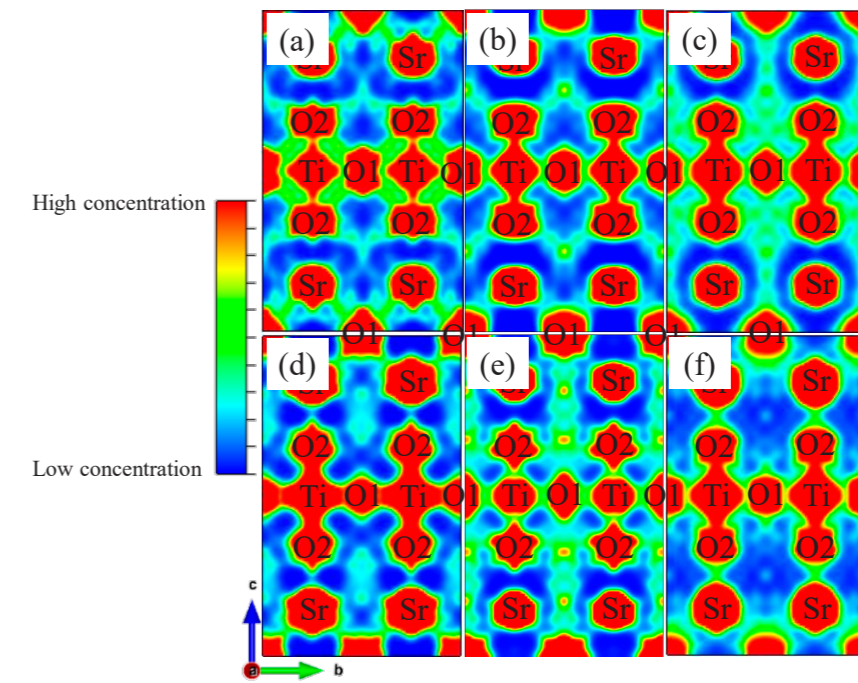
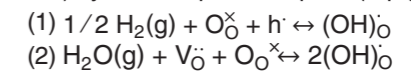


Figure 2: Electron density distributions on the (200) planes of (a) as-sintered, (b) moist-reduction-annealed, and (c) reduced STF10 and (d) as-sintered, (e) moist-reduction-annealed, and (f) reduced STA05. Reprinted from Yagi *et al.* [1] with permission from Elsevier.

Figure 2 shows the electron density distributions on the (200) planes of STF10 and STA05, which were obtained by the maximum entropy method. The electron density distribution on reduced STF10 extended more widely than that on reduced STA05. This result suggests that reduced STF10 has a higher electrical conductivity than reduced STA05 at low temperatures. The result suggests that STA05 had a larger proton transport number than STF10 at low temperatures. The electron density distributions between an O2 site and its nearest-neighbor O2 site in reduced STF10 and moist-reduction-annealed STA05 were denser than those of the other samples. These results suggest that protons appear in the space between the two O2 sites in the reduced STF10 and moist-reduction-annealed STA05. Thus, it was possible to detect protons in the oxides with proton defects, although we investigated synchrotron X-ray powder diffraction only and then calculated electron density distributions, meaning that neutron diffraction is not always needed. The electron density distributions between the two O2 sites were not so dense for moist-reduction-annealed STF10 and reduced STA05. On the basis of all the results, we conclude that proton defects were introduced to the Fe-doped sample (STF10) by a redox reaction (eq. (1)) and to the Al-doped sample

(STA05) by water vapor absorption (eq. (2)) [1]:



Thus, the mechanism of proton defect introduction was different between Fe and Al as the acceptor dopants for the Sr_2TiO_4 -based layered perovskites. The conclusion is a guide for material selection when developing new proton-conductive oxides with greater amounts of proton defects. For this study, the electron density distribution obtained from SXRPD was useful to investigate proton defects introduced in the proton conductive oxides.

REFERENCES

- [1] Y. Yagi, I. Kagomiya and K. Kakimoto, *Solid State Sci.* **108**, 106407 (2020).
- [2] H. Toraya, H. Hibino and K. Ohsumi, *J. Synchrotron Radiat.* **3**, 75 (1996).
- [3] F. Izumi and K. Momma, *Solid State Phenom.* **130**, 15 (2007).
- [4] R. D. Shanon, *Acta Cryst. A* **32**, 751 (1976).

BEAMLINE

BL-4B2

Y. Yagi, I. Kagomiya and K. Kakimoto (Nagoya Inst. of Tech.)